

UC Irvine

UC Irvine Previously Published Works

Title

Development of brain white matter and math computation ability in children born very preterm and full-term.

Permalink

<https://escholarship.org/uc/item/4jn0b4sj>

Authors

Collins, Simonne

Thompson, Deanne

Kelly, Claire

et al.

Publication Date

2021-10-01

DOI

10.1016/j.dcn.2021.100987

Peer reviewed



Development of brain white matter and math computation ability in children born very preterm and full-term

Simonne E. Collins^{a,b,c}, Deanne K. Thompson^{b,c,d,e}, Claire E. Kelly^{a,b,c}, Joseph Y.M. Yang^{c,d,f,g},
Leona Pascoe^{a,b}, Terrie E. Inder^{b,h}, Lex W. Doyle^{b,d,i,j,k}, Jeanie L.Y. Cheong^{b,i,j,k},
Alice C. Burnett^{b,d,k,l}, Peter J. Anderson^{a,b,*}

^a Turner Institute for Brain and Mental Health, Monash University, Melbourne, Australia

^b Victorian Infant Brain Study (VIBeS), Murdoch Children's Research Institute, Melbourne, Australia

^c Developmental Imaging, Murdoch Children's Research Institute, Melbourne, Australia

^d Department of Paediatrics, The University of Melbourne, Melbourne, Australia

^e Florey Institute of Neuroscience and Mental Health, Melbourne, Australia

^f Neuroscience Advanced Clinical Imaging Suite (NACIS), Department of Neurosurgery, The Royal Children's Hospital, Melbourne, Australia

^g Neuroscience Research, Murdoch Children's Research Institute, Melbourne, Australia

^h Department of Pediatric Newborn Medicine, Brigham and Women's Hospital, Harvard Medical School, Boston, USA

ⁱ Newborn Research, The Royal Women's Hospital, Melbourne, Australia

^j Department of Obstetrics and Gynaecology, The University of Melbourne, Melbourne, Australia

^k Premature Infant Follow-Up Program, Royal Women's Hospital, Melbourne, Australia

^l Neonatal Medicine, Royal Children's Hospital, Melbourne, Australia

ARTICLE INFO

Keywords:

Preterm birth

Arithmetic

Academic performance

Microstructure

Diffusion imaging

Magnetic resonance imaging

ABSTRACT

Children born very preterm (VPT; <32 weeks' gestation) have alterations in brain white matter and poorer math ability than full-term (FT) peers. Diffusion-weighted magnetic resonance imaging studies suggest a link between white matter microstructure and math in VPT and FT children, although longitudinal studies using advanced modelling are lacking. In a prospective longitudinal cohort of VPT and FT children we used Fixel-Based Analysis to investigate associations between maturation of white matter fibre density (FD), fibre-bundle cross-section (FC), and combined fibre density and cross-section (FDC) and math computation ability at 7 ($n = 136$ VPT; $n = 32$ FT) and 13 ($n = 130$ VPT; $n = 44$ FT) years, as well as between change in white matter and math computation ability from 7 to 13 years ($n = 103$ VPT; $n = 21$ FT). In both VPT and FT children, higher FD, FC and FDC in visual, sensorimotor and cortico-thalamic/thalamo-cortical white matter tracts were associated with better math computation ability at 7 and 13 years. Longitudinally, accelerated maturation of the posterior body of the corpus callosum (FDC) was associated with greater math computation development. White matter-math associations were similar for VPT and FT children. In conclusion, white matter maturation is associated with math computation ability across late childhood, irrespective of birth group.

1. Introduction

Many children born very preterm (VPT; <32 weeks' gestational age [GA]) have academic challenges, particularly in math (Aarnoudse-Moens et al., 2009; Twilhaar et al., 2018). Math ability is associated with better economic, social and psychological outcomes well into adulthood (Parsons and Bynner, 2005). In individuals born preterm, poor math ability in childhood has been shown to be negatively associated with five different wealth indicators at age 42 years, independent of educational

qualifications (Basten et al., 2015).

Complex neural systems are utilised for developing math skills and completing math tasks (Arsalidou et al., 2018; Peters and De Smedt, 2018). Furthermore, evidence suggests that the neural associations of math change across development with age and experience (Cantlon et al., 2009; Rivera et al., 2005; Rosenberg-Lee et al., 2011). The association between white matter properties and math ability is particularly relevant for children born VPT because alterations in white matter are common in this population (Nosarti et al., 2014; Thompson et al., 2014;

* Corresponding authors at: Turner Institute for Brain and Mental Health, Monash University, Melbourne, Australia.

E-mail addresses: simonne.collins@monash.edu (S.E. Collins), peter.j.anderson@monash.edu (P.J. Anderson).

<https://doi.org/10.1016/j.dcn.2021.100987>

Received 15 September 2020; Received in revised form 7 July 2021; Accepted 11 July 2021

Available online 12 July 2021

1878-9293/© 2021 The Authors.

Published by Elsevier Ltd.

This is an open access article under the CC BY-NC-ND license

(<http://creativecommons.org/licenses/by-nc-nd/4.0/>).

Vangberg et al., 2006), with evidence of delayed white matter development in many white matter tracts, including the corona radiata, corpus callosum, forceps major, and the inferior and superior longitudinal fasciculi (Kelly et al., 2016; Li et al., 2015). The microstructural organization of these tracts is associated with math ability in typically developing children ranging from 7 to 18 years (Li et al., 2013; Matejko et al., 2013; Peters and De Smedt, 2018; van Eimeren et al., 2008) and alterations have been observed in children with dyscalculia (Rykhlevskaia et al., 2009). White matter microstructural and macrostructural anatomy can be modelled *in vivo* using diffusion magnetic resonance imaging (MRI). Diffusion MRI studies have the potential to help us better understand the neural mechanisms underlying poor math ability in VPT individuals.

A common diffusion model used to investigate white matter microstructure is diffusion tensor imaging (DTI), generating measures such as fractional anisotropy (FA). However, FA cannot differentiate between axonal alterations (such as reduced axonal diameter and reduced axonal packing densities) and the effects of crossing fibres and other complex fibre arrangements. In comparison, Neurite Orientation Dispersion and Density Imaging (NODDI), a compartmental model, enables investigation of more complex white matter microstructural organization, providing measures of axonal orientation dispersion and axonal density (Zhang et al., 2012). By performing a Tract-Based Spatial Statistics analysis of DTI and NODDI metrics, our group reported that math computation ability was positively associated with FA in widespread white matter tracts in 7-year-olds born VPT (Kelly et al., 2016), including the corona radiata, corpus callosum, forceps major and the inferior and superior longitudinal fasciculi, as well as with FA and axonal density in similar tracts in both VPT and full-term born (FT; ≥ 37 weeks' GA) children at 13 years of age (Collins et al., 2019). However, these associations did not differ between VPT and FT children. In contrast, previous studies have reported differences between VPT and FT groups for associations between white matter microstructure and general intelligence, executive function and reading, in terms of associated tracts and direction of association (Bruckert et al., 2019; Travis et al., 2016; Vollmer et al., 2017).

Although compartmental models such as NODDI improve estimates of white matter microstructure compared to DTI, they remain limited to the voxel level and the anatomical specificity of results are compromised. In contrast, the recently developed fixel-based analysis (FBA) framework models white matter microstructure and macrostructure at the level of each individual fibre population within a voxel, termed a 'fixel' (Raffelt et al., 2017). For each fixel, FBA estimates three white matter properties: 1. the microscopic density of axons within the fibre population (fibre density, FD); 2. the macroscopic cross-sectional area that the fibre population occupies (fibre-bundle cross-section, FC); and, 3. a combined measure encompassing both of these microstructural and macrostructural properties (fibre density and cross-section, FDC; Raffelt et al., 2017). Typically, FBA metrics in the white matter increase throughout childhood (Genc et al., 2018). VPT infants (Pannek et al., 2018) and children (Kelly et al., 2020) have widespread lower FD, FC and FDC compared with term controls, and we recently found that the increase in FDC specifically in parts of the corpus callosum and corticospinal tract over the 7 to 13-year time period was comparatively slower in VPT children than FT peers (Kelly et al., 2020). The FBA metrics at term-equivalent age have been positively associated with cognitive and motor outcomes in VPT children at 12 and 24-months of age (Pannek et al., 2020), but it remains to be investigated whether FBA alterations in VPT children underpin their poorer math ability.

The aims of the current study were two-fold. First, we aimed to investigate whether the cross-sectional relationship between math computation ability and FBA estimates of white matter microstructure and macrostructure differed between VPT and FT children at 7 and 13 years. While we expected to find positive associations between math computation ability and FD, FC and FDC in FT children in the corona radiata, corpus callosum, forceps major and inferior and superior

longitudinal fasciculi, we expected the pattern of associated tracts to differ in VPT children. Second, we aimed to investigate how the maturation of white matter microstructure and macrostructure from 7 to 13 years is associated with the development of math computation ability across the same time period, and whether this relationship differed between VPT and FT children. We hypothesised that greater increases in all FBA metrics would be associated with greater improvement in math computation ability for both VPT and FT children but that there may be regional variations between groups.

2. Method

2.1. Participants and procedure

224 VPT infants (<30 week's GA or <1250 g birth weight) and 45 FT infants (≥ 37 weeks' GA) were recruited in 2001–2003 at the Royal Women's Hospital, Melbourne and form the prospective longitudinal Victorian Infant Brain Study (ViBeS). Infants with genetic or congenital abnormalities were excluded. A further 31 FT participants were recruited from Maternal Child Health Centres at age 2 years and matched to VPT participants based on socio-demographic details. At 7 years (corrected for prematurity; Wilson-Ching et al., 2014), 197 VPT and 69 FT children returned for follow up (88 % and 90 %, respectively), and at 13 years (corrected for prematurity) 179 VPT and 61 FT children were followed up (80 % and 79 %, respectively). A total of 176 VPT and 60 FT children attended both the 7 and 13-year follow ups.

At each follow up participants completed a battery of neuropsychological assessments and were offered an MRI. The 31 FT participants recruited at 2 years were only offered an MRI at 13 years. Ethics approval was obtained from the Human Research Ethics Committee at the Royal Children's Hospital, Melbourne. Parents/guardians provided written informed consent and children provided verbal assent at each follow-up.

2.2. Measures

2.2.1. Math computation ability

To assess math computation ability at both 7 and 13 years, children completed the Math Computation subtest from the Wide Range Achievement Test – 4th edition (WRAT-4; Wilkinson and Robertson, 2006), which is appropriate for ages 5 years and older. At 7 years, children begin with 15 'oral math' questions including counting and single digit addition and subtraction word problems, before moving to 40 written calculation problems that increase in difficulty. Written problems include addition, subtraction, multiplication, division and algebra. At 13 years, children are required to complete only the written problems, unless they fail to answer at least 5 problems correctly, in which case they are then asked the 'oral math' questions. Children were instructed to complete as many written items as possible within 15 min. In order to assess each child's individual development in computation ability over time, we used participants' raw scores in analyses, with higher scores reflecting better ability.

2.2.2. IQ

At 7 years, IQ was estimated using the 4-subtest version of the Wechsler Abbreviated Scale of Intelligence (WASI; Wechsler, 1999). At 13 years, IQ was estimated using the composite score of the Kaufman Brief Intelligence Test – 2nd edition (KBIT-2; Kaufman and Kaufman, 2004). Both measures include estimates of verbal and non-verbal IQ, with a mean of 100 and standard deviation of 15 (higher scores reflect better performance).

2.2.3. Social risk

At 7 and 13 years, parents provided details on a questionnaire relating to six domains: 1) family structure, 2) primary caregiver education level, 3) employment and 4) income status of the primary income

earner, 5) maternal age at birth and 6) level of English spoken at the time of recruitment. To compute a Social Risk Index score, the 6 domains were scored 0, representing the lowest risk, to 2, representing the highest risk (Roberts et al., 2008). The maximum possible score is 12. The Social Risk Index score was then categorised around the median, as lower (0–1) or higher (2–12) social risk (Roberts et al., 2008). Where social risk information was missing it was imputed based on their score from the previous timepoint. One VPT participant had no social risk information at any timepoint and was excluded.

2.2.4. MRI acquisition

At both 7 and 13 years, scans were completed following mock MRI training at the Royal Children's Hospital, Melbourne, using a Siemens Magnetom Trio, Tim System 3 T scanner. At 7 years the diffusion weighted imaging (DWI) sequence was acquired with a b -value = 3000 s/mm^2 , 45 noncollinear gradient directions in total, $6 b = 0 \text{ s/mm}^2$ images, TR = 7,400 ms, TE = 106 ms, FOV = 240×240 mm, matrix = 104×104 and an isotropic voxel size of 2.3 mm^3 . A T_1 -weighted sequence was also acquired with TR = 1900 ms, TE = 2.27 ms, FOV = 210×210 mm, matrix = 256×256 , flip angle = 9° and 0.8 mm isotropic voxels. At 13 years, the DWI sequence was acquired with a b -value = 2800 s/mm^2 , 60 diffusion-weighted gradient directions, $4 b = 0 \text{ s/mm}^2$ images, TR = 3200 ms, TE = 110 ms, FOV = 260×260 mm, matrix = 110×110 and an isotropic voxel size of 2.4 mm^3 . Additionally, a pair of $b = 0 \text{ s/mm}^2$ images were acquired with reversed phase encoding. A T_1 -weighted sequence was also acquired with TR = 2530 ms, TE = 1.77, 3.51, 5.32, 7.2 ms, FOV = 230×209 mm, matrix = 256×230 , interpolated 256×256 , flip angle = 7° and 0.9 mm isotropic voxels.

2.2.5. DWI pre-processing

Diffusion weighted images (DWI) underwent susceptibility-induced distortion correction at 7 years using BrainSuite version 18, based on T_1 -weighted images (Bhushan et al., 2012), and at 13 years using the Functional MRI of the Brain Software Library (FSL; version 5.0.11) 'topup' tool based on availability of reversed phase-encoded images (Andersson et al., 2003). For both timepoints, images underwent correction for eddy currents and motion using the FSL 'eddy' tool (Andersson et al., 2017, 2016; Andersson and Sotiropoulos, 2016). The b -vectors were rotated for use in subsequent steps (Leemans and Jones, 2009). Corrected DWI were visually inspected and quantitative quality control metrics were obtained using the FSL Quality Assessment for DMRI (QUAD) and Study-wise QUality Assessment for DMRI (SQUAD) tools (Bastiani et al., 2018). Quality control metrics were similar between the VPT and FT groups, although the 7-year images generally had higher motion metrics than the 13-year images (Kelly et al., 2020). Corrected images were brain extracted using the FSL Brain Extraction Tool (BET; Smith, 2002).

2.2.6. Fixel-based analysis

Preprocessed images were analysed as per recommendations for a single-shell, single-tissue FBA in MRtrix3, version 3.0_RC3 (Tournier et al., 2019). This involved bias field correction (Tustison et al., 2010), global intensity normalisation, upsampling to 1.3 mm isotropic voxels, and constrained spherical deconvolution (Tournier et al., 2013) using an average response function derived from all participants' images. Separate 7-year and 13-year fibre orientation distribution (FOD) templates were generated from a randomly selected subset of 30 images per timepoint (15 VPT without major neonatal brain abnormalities and 15 FT). A longitudinal template was also created using the total 60 images from both timepoints. Age and sex of the template subsets did not differ from the larger sample (all $p > 0.1$). 7-year FOD images were registered to the 7-year template, 13-year FOD images were registered to the 13-year template, and all FOD images were registered to the longitudinal template (Raffelt et al., 2012, 2011). FODs were segmented to estimate fixels, and FBA metrics (FD, FC, FDC) were then computed (Raffelt

et al., 2017). The FC metric was log transformed prior to analyses being undertaken (Raffelt et al., 2017). Whole-brain tractography was performed on the templates, and tractograms underwent spherical-deconvolution informed filtering of tractograms (SIFT; Smith et al., 2013). Image analysis steps have been detailed previously (Kelly et al., 2020).

2.2.7. Statistical analysis

Perinatal and demographic characteristics, as well as neurodevelopmental (math computation ability and estimated IQ) outcomes, were compared between the VPT and FT participants using independent samples t -tests and chi-square models for continuous and categorical variables, respectively, in Stata 16 (StataCorp, 2019).

Perinatal and neurodevelopmental variables were compared between those that were included in the current study at each follow up (participants) and those that were recruited at birth but were not included in the current study (non-participants) using independent samples t -tests and chi-square models in Stata 16.

Statistical analyses of FBA metrics were completed at every fixel across the brain white matter using general linear modelling and connectivity-based fixel enhancement (CFE) in MRtrix3 (Raffelt et al., 2015). Multiple comparisons were controlled for using non-parametric permutation testing ($n = 5000$), assigning a family-wise error rate (FWE)-corrected p -value to each fixel (Nichols and Holmes, 2002).

To address aim one, we investigated whether the cross-sectional associations between each FBA metric and math computation ability (i.e. 7-year FBA metric and 7-year math; and 13-year FBA metric and 13-year math) differed between VPT and FT children using an interaction model. This was adjusted for age at assessment and social risk. Secondary analyses were undertaken excluding children with an IQ < 70 at the time of assessment, ensuring low intelligence was not a confounding factor. We also investigated whether the relationships between FBA metrics and math computation ability differed between males and females using an interaction model. When no significant interactions were identified, all participants were combined to examine associations between FBA metrics and math computation ability in the total sample. Cross-sectional analyses were performed in the relevant cross-sectional template space.

To address aim 2, we investigated whether the change in FBA metrics over time (calculated by subtracting the 7-year images from the 13-year images) was associated with development in math computation ability over time (calculated by subtracting the 7-year score from the 13-year score). This was adjusted for baseline math computation ability at 7 years, the number of years between assessments and social risk at 7 years. Secondary analyses were undertaken excluding children with an IQ < 70 at either 7 or 13 years. Two interaction models were constructed to explore whether the relationship between the change in FBA metrics and change in math computation ability differed between VPT and FT children, or between males and females. Longitudinal analyses were performed in the longitudinal template space using a modified version of CFE (Genc et al., 2018; Kelly et al., 2020).

In line with previous work (Kelly et al., 2020; Pecheva et al., 2019), for each aim we ran additional sensitivity analyses for the FC and FDC metrics adjusting for intracranial volume (ICV; generated from T_1 -weighted images using Statistical Parametric Mapping, version 12 and log transformed; Smith et al., 2019). For the longitudinal analyses, this sensitivity analysis was performed adjusting for the log value of the change in ICV over time. At the 7-year timepoint, some participants had excessive motion artefacts on their T_1 -weighted image and ICV data was unable to be extracted, therefore, these participants were excluded from sensitivity analyses adjusting for ICV at 7-years and in the longitudinal analyses.

Additionally, at the 7-year timepoint, a subset of images ($\sim 30\%$) were acquired with non-uniform gradient directions and we therefore repeated the 7-year and longitudinal analyses excluding these participants, to examine whether results were influenced by this subset (Kelly

et al., 2016).

Fixels were considered statistically significant at $p < 0.05$, FWE-corrected. Significant fixels were anatomically localised by visual inspection with reference to a white matter atlas (Oishi et al., 2011), with confirmation by a paediatric neurosurgery research fellow, experienced in white matter tract anatomy and tractography research (JYMY).

3. Results

3.1. Participant characteristics

At 7 years, 159 VPT and 35 FT children had an MRI, with 136 VPT and 32 FT children having sufficient data for inclusion in the FBA analyses (representing 61 % and 42 % of the original samples, respectively). At 13 years, 141 VPT and 47 FT children had an MRI, with 130 VPT and 44 FT children included in the FBA analyses (representing 58 % and 58 % of the original samples, respectively). The longitudinal analyses included 103 VPT and 21 FT participants (representing 46 % and 28 % of the original samples, respectively). For exclusions at each timepoint and a participant flow chart see Supplementary Fig. S1.

Perinatal and demographic characteristics and neurodevelopmental outcomes in VPT and FT participants are reported in Table 1. There were no differences between groups for age at assessment or sex. As we have reported elsewhere (Collins et al., 2019), VPT children had lower math computation ability, a lower estimated IQ and were more often from a higher social risk background than FT children (Table 1).

Perinatal and neurodevelopmental characteristics of participants

and non-participants are reported in Supplementary Table S1. VPT participants were more likely to have been from a multiple birth and less likely to have had a postnatal infection and moderate-to-severe white matter abnormalities at term-equivalent age, compared with VPT non-participants (see Supplementary Table S1). The math computation and estimated IQ of VPT participants were significantly higher at 7 years compared with VPT non-participants, though this was not the case at 13 years. For the longitudinal analyses, VPT participants had a higher estimated IQ at 7 years compared with VPT non-participants (see Supplementary Table S1). FT participants were similar to FT non-participants on most perinatal characteristics. However, FT participants in the longitudinal analysis had a slightly younger GA at birth than FT non-participants (*mean difference* = 0.67 weeks [95 % confidence interval, 0.01–1.33], $p = 0.047$). There were no differences in math computation or estimated IQ scores between FT participants and non-participants.

3.2. Cross-sectional associations between FBA metrics and math computation ability

There were no group differences in FBA-math associations between VPT and FT children at either timepoint. There were also no differences in FBA-math associations between males and females. Thus, associations between FBA metrics and math computation ability are reported for the total sample. There were no negative associations between FBA metrics and math computation ability, thus all associations reported are in the positive direction.

Table 1

Demographic and perinatal characteristics of VPT and FT participants included in the 7-year, 13-year and longitudinal analyses.

	7 years		13 years		Longitudinal	
	VPT <i>n</i> = 136	FT <i>n</i> = 32	VPT <i>n</i> = 130	FT <i>n</i> = 44	VPT <i>n</i> = 103	FT <i>n</i> = 21
Age (years) at assessment ^a , <i>M</i> (<i>SD</i>) range	7.52 (0.23) 6.8–8.1	7.58 (0.22) 7.1–8.1	13.23 (0.38) 11.8–14.9	13.21 (0.45) 12.3–14.3	5.68 ^b (0.42) 4.2–7.4	5.78 ^b (0.44) 5.2–6.7
Female, <i>n</i> (%)	69 (51)	17 (53)	61 (47)	23 (52)	52 (50)	10 (48)
Gestational age (weeks), <i>M</i> (<i>SD</i>)	27.5 (1.9)	39.0 (1.3)	27.4 (1.9)	39.0 (1.4)	27.5 (1.9)	38.7 (1.2)
Birthweight (g), <i>M</i> (<i>SD</i>)	977 (224)	3247 (509)	964 (230)	3303 (551)	975 (230)	3273 (549)
SGA, <i>n</i> (%)	11 (8)	1 (3)	11 (9)	0	9 (9)	0
Multiple pregnancy, <i>n</i> (%)	65 (48)	2 (6)	63 (48)**	4 (9)	54 (52)**	2 (9)
BPD, <i>n</i> (%)	40 (29)	–	42 (32)	–	29 (28)	–
PDA, <i>n</i> (%)	66 (49)	–	61 (47)	–	51 (49)	–
Postnatal infection ^c , <i>n</i> (%)	43 ^d (32)	–	42 ^e (33)	–	31 ^d (31)	–
Grade III/IV IVH, <i>n</i> (%)	5 (4)	–	7 (5)	–	5 (5)	–
Cystic PVL, <i>n</i> (%)	4 (3)	–	4 (3)	–	4 (4)	–
Moderate-to-severe WMA, <i>n</i> (%)	18 ^f (13)	–	17 (13)	–	13 (13)	–
Math raw score, <i>M</i> (<i>SD</i>), range	19.2 (4.9)* 4–33	21.4 (3.4) 12–28	34.7 (7.3)** 13–53	39.0 (6.8) 27–54	16.1 ^g (4.9)** –2 ^h –27	19.8 ^g (3.5) 13–25
Math standard score, <i>M</i> (<i>SD</i>), range	92.1 (17.3)* 55–144	99.1 (14.6) 61–129	92.1 (15.8)* 55–140	101.6 (15.3) 77–144	1.3 ^g (11.9) –36–25	5.2 ^g (11.3) –22–24
Low math score ^e , <i>n</i> (%)	46 (34)*	4 (12.5)	45 (35)*	8 (18)	–	–
IQ, <i>M</i> (<i>SD</i>)	99.2 (12.6)**	109.1 (11.4)	99.6 (18.0)**	110.0 (12.5)	99.1 ^j (12.8)**	110.5 ^j (11.5)
IQ < 70, <i>n</i> (%)	1 (<1 %)	0	9 (7)	0	6 ^k (5)	0
Higher social risk background, <i>n</i> (%)	79 (58)*	9 (28)	78 (60)*	16 (36)	58 ^l (56)*	5 ^l (24)

n = number of participants, *M* = mean, *SD* = standard deviation, SGA = small for gestational age, BPD = bronchopulmonary dysplasia, PDA = patent ductus arteriosus, IVH = intraventricular haemorrhage, WMA = white matter abnormality, PVL = periventricular leukomalacia.

* *p*-value < 0.05.

** *p*-value < 0.001.

^a Corrected for prematurity.

^b Represents the number of years between assessment at each timepoint.

^c Defined as a confirmed case of sepsis or necrotising enterocolitis.

^d 2 missing data points.

^e 3 missing data points.

^f 1 missing data point.

^g Represents change in math computation ability from 7 to 13 years.

^h One child scored 2 points lower at 13 years than at 7 years. They had an IQ < 70 at 13 years and were excluded from the secondary IQ analyses.

ⁱ Defined as a score >1 SD (15) below the normative test mean (100).

^j Estimated IQ at 7 years.

^k Number of children with IQ < 70 at either 7 or 13 years.

^l Represents social risk background at 7 years.

3.2.1. 7-year associations

3.2.1.1. FD. Significant associations were observed in a small number of fixels ($n = 370$; 0.07 % of the total number of fixels in the white matter template analysis fixel mask). The location of these fixels included the: i) corticospinal tract from the level of the internal capsule in the left hemisphere and from the level of the cerebral peduncle in the right hemisphere, through to the brain stem; ii) left inferior fronto-occipital fasciculus; and iii) splenium of corpus callosum (including the right forceps major; see Fig. 1 and Supplementary Table S2 for more detail; see Supplementary Fig. S2 for p -values of significant fixels). These results were similar after excluding the child with an IQ < 70 (Supplementary Fig. S3, Supplementary Table S3). No significant fixels remained after excluding the images acquired with non-uniform gradient directions.

3.2.1.2. FC and FDC. Significant associations were identified in 17,744 (3.4 %) fixels for FC, and 8,005 (1.5 %) fixels for FDC, both of which occupied similar anatomical regions (Fig. 1 and Supplementary Table S2; see Supplementary Fig. S2 for p -values of significant fixels). They included: i) bilateral corticospinal tracts following their entire intracranial course; ii) bilateral superior corona radiata; iii) bilateral somatosensory fibres traversing through the posterior limbs of the internal capsules and into the thalami; iv) the posterior body of the corpus callosum (including the isthmus); v) both inferior fronto-occipital fasciculi traversing through the external capsules (predominantly left lateralised); and the pontine crossing tract and bilateral middle cerebellar peduncles. A specific association was identified with FDC in the anterior thalamic radiations (predominantly left lateralised). Results were similar after excluding the child with an IQ < 70 (Supplementary Fig. S3, Supplementary Table S3). Results were also similar, although the spatial extent reduced slightly, after adjusting for ICV (Supplementary Fig. S4, Supplementary Table S3). No significant associations remained after excluding the images acquired with non-uniform gradient directions.

3.2.2. 13-year associations

3.2.2.1. FD. Significant associations were observed in 1,070 fixels (0.2 %), located in the: i) brainstem portion of the right corticospinal tract; ii) right anterior thalamic radiation; iii) posterior body, splenium and tapetum of the corpus callosum; iv) bilateral superior corona radiata (Fig. 1 and Supplementary Table S2; see Supplementary Fig. S2 for p -values of significant fixels). Many of the same regions remained associated after excluding the children with an IQ < 70 (Supplementary Fig. S3, Supplementary Table S4).

3.2.2.2. FC and FDC. Associations were identified in 29,100 (5.0 %) fixels for FC and 17,710 (3.0 %) fixels for FDC, in similar regions for both parameters (Fig. 1 and Supplementary Table S2; see Supplementary Fig. S2 for p -values of significant fixels). Associations were observed in: i) both corticospinal tracts along the entire intracranial course; ii) bilateral corona radiata; iii) bilateral anterior thalamic radiations; iv) bilateral somatosensory fibres in the posterior limbs of the internal capsules and thalami (left lateralised for FDC); v) the callosal genu (including forceps minor), posterior body (including the isthmus), and splenium (including forceps major; right lateralised for FC); vi) the cingulum (right lateralised for FC); vii) bilateral inferior fronto-occipital fasciculus through the external capsules; viii) and the middle cerebellar peduncles. Specific associations were identified with FC in the pontine crossing tract and the anterior commissure, and with FDC in the callosal tapetum fibres and the hippocampal portion of the cingulum. Significant associations remained in most regions after excluding the children with an IQ < 70 (Supplementary Fig. S3, Supplementary Table S4). These results largely reduced after controlling for ICV (Supplementary Fig. S4, Supplementary Table S4).

3.3. Longitudinal associations

As with the cross-sectional analyses, there were no group differences in FBA-math associations between VPT and FT children or between males and females. Therefore, all participants were combined for the longitudinal analyses. We found no significant associations between change in FD or FC and development in math computation ability from 7

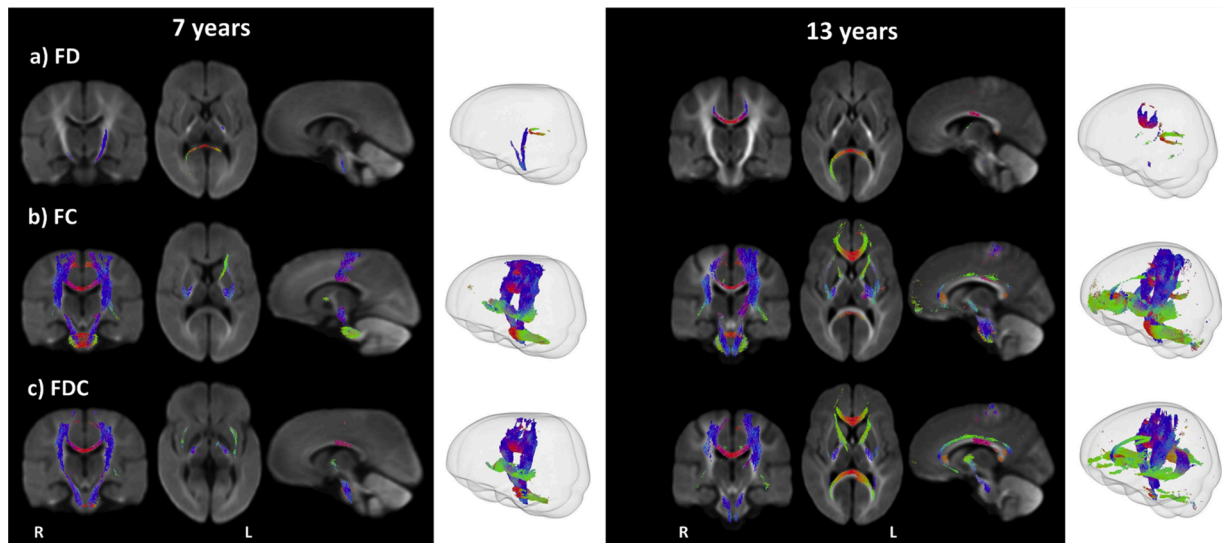


Fig. 1. Images illustrate regions where there were cross-sectional associations between math computation ability and fixel-based analysis metrics [a) fibre density (FD), b) fibre-bundle cross-section (FC), and c) combined fibre density and cross-section (FDC)] at 7 years (left panel) and 13 years (right panel). Results are adjusted for age at assessment and social risk. Results are presented as fibre tracts (streamlines) passing through significant fixels ($p < 0.05$, FWE-corrected). Streamlines are coloured by direction: red: left-right; green: anterior-posterior; blue: inferior-superior. In the first three columns of each panel, streamlines are presented as 2D slices overlaid on the template image. In the final column, streamlines are presented in 3D in glass brain representations (Mito et al., 2018). (For interpretation of the references to colour in this figure legend, the reader is referred to the web version of this article).

to 13 years (calculated as 13 year math score minus 7 year math score).

Increases in FDC in a small number of fixels ($n = 56$, 0.01 %) in the posterior body of corpus callosum were positively associated with development in math computation ability (Fig. 2, Supplementary Table S2; see Supplementary Fig. S5 for p -values for significant fixels), which remained present after controlling for ICV and after excluding children whose 7-year images were acquired with non-uniform gradient directions (Supplementary Fig. S6, Supplementary Table S5), but not after excluding children with an IQ < 70 at either age.

4. Discussion

Using FBA, this study found that higher FD, FC and FDC, predominantly in visual, sensorimotor and cortico-thalamic/thalamic-cortical tracts, were associated with better math computation ability in 7 and 13-year-old children. Increasing values of FDC in the posterior body of the corpus callosum from 7 to 13 years (i.e. increasing maturation) were associated with greater improvement in math computation ability. VPT children had similar associations between math computation and white matter microstructure and macrostructure to their FT peers.

Contrary to our hypothesis, the relationships between longitudinal white matter development in FBA metrics and development in math computation ability did not differ between VPT and FT children. Other studies have reported that VPT children rely on different white matter systems for reading (Bruckert et al., 2019; Travis et al., 2016), executive function and general intelligence (Vollmer et al., 2017) compared with FT peers, but this does not appear to be the case for math computation. We have previously reported no birth group differences in the association between white matter microstructure and math computation in this cohort at age 13 years using voxel-wise analysis of DTI and NODDI metrics (Collins et al., 2019). The current study confirms this finding, using the more specific FBA framework and incorporating data from 7 and 13 years. However, we caution that the VPT study sample may not be representative of the original birth cohort as participants had higher math computation scores and were less likely to have moderate-to-severe white matter abnormalities at term-equivalent age than participants without FBA data. It remains possible that examining more foundational math skills (i.e., magnitude processing or fact retrieval) may uncover group differences in these associations, although to date the examination of these more foundational skills in the preterm

population is limited (Simms et al., 2015).

In the total sample of VPT and FT children, we found converging evidence for associations between white matter microstructure and macrostructure, and math computation ability at 7 and 13 years. Much of the previous literature investigating the association between math and brain white matter must be interpreted with caution as analyses have utilised voxel-level estimates of diffusion, limiting the anatomical specificity and biological interpretability of findings. FD, FC and FDC were all associated with math computation ability in the current study, suggesting that increased cross-sectional area of specific white matter tracts, in conjunction with higher axonal density, is associated with better math computation ability in childhood (Pannek et al., 2020).

Associations were present in tracts important for processing visual stimuli. More specifically, the fixel-based measures in the splenium of the corpus callosum along with the callosal fibres making up the forceps major, and inferior fronto-occipital fasciculi were associated with math computation ability at both 7 and 13 years. These associations are concordant with previous DTI investigations showing positive associations of FA in these tracts with math in our VPT cohort (Collins et al., 2019; Kelly et al., 2016) and in typically developing children (Li et al., 2013) and adolescents (Matejko et al., 2013), with reduced FA evident in children with dyscalculia compared with peers (Rykhlevskaia et al., 2009). Axonal density in the splenium, estimated with NODDI, has also been positively associated with math computation in our cohort of VPT and FT children at 13 years (Collins et al., 2019). The splenium and forceps major provide interhemispheric connections between visual cortical regions (Dougherty et al., 2005; Hofer and Frahm, 2006; Putnam et al., 2010); while the inferior fronto-occipital fasciculi provide intrahemispheric connections between cortical regions associated with visual and verbal processing of numeric information (Dehaene et al., 2003; Shum et al., 2013), arithmetic fact retrieval (Grabner et al., 2009) and domain-general skills such as working memory (Klein et al., 2018). Our work suggests that children with better math computation ability have greater overall axonal development (i.e. increased FD, FC and FDC) in these tracts, which may in turn enhance their capacity for the integration of multi-modal numeric information and domain-general processing, including working memory.

We found consistent evidence for associations with math computation across FBA metrics at both timepoints in white matter tracts implicated in the sensorimotor network, including the corticospinal

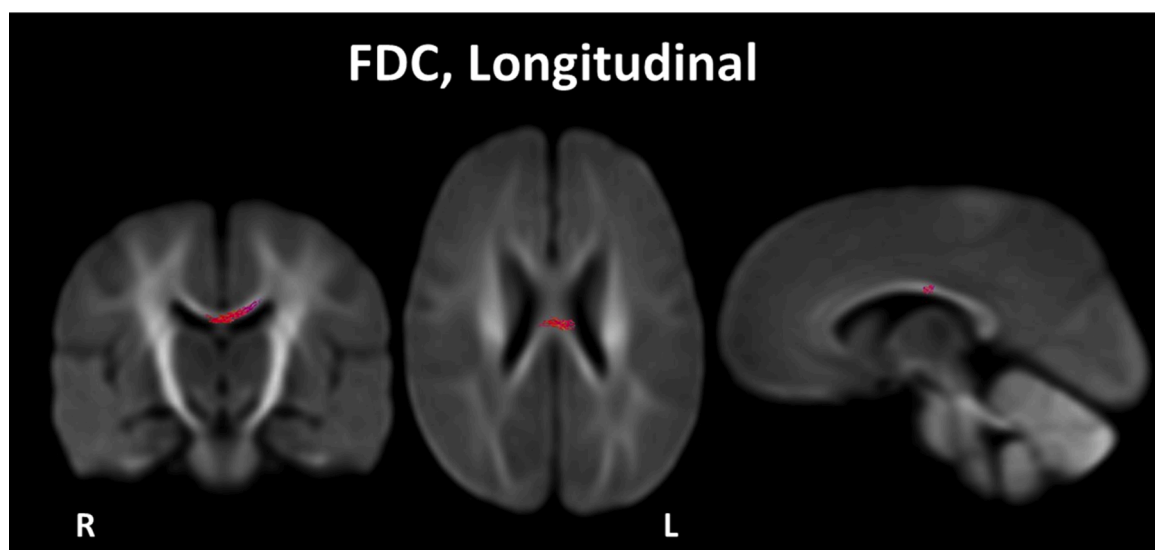


Fig. 2. Images illustrate regions where development in math computation ability from 7 to 13 years was associated with increases in combined fibre density and cross-section (FDC) from 7 to 13 years, adjusted for math computation ability at 7 years, the number of years between assessments and social risk at 7 years. Results are presented as fibre tracts (streamlines) passing through significant fixels ($p < 0.05$, FWE-corrected). Streamlines are coloured by direction: red: left-right. (For interpretation of the references to colour in this figure legend, the reader is referred to the web version of this article).

tract and superior corona radiata, and the posterior body and isthmus of the corpus callosum. Similar cross-sectional findings have been reported in DTI studies, whereby positive FA-math associations have been identified in the bilateral corticospinal tract for adolescents (Matejko et al., 2013) and in the left superior corona radiata in our previous VPT investigations (Collins et al., 2019; Kelly et al., 2016), in typically developing children (van Eimeren et al., 2008) and adolescents (Matejko et al., 2013). Conversely, reduced FA in the right corticospinal tract has been observed in children with dyscalculia compared to peers (Rykhlevskaia et al., 2009). The functional relevance of the sensorimotor tracts for math is less clear than for the visual pathways. It has been hypothesised, however, that as the left superior corona radiata is commonly associated with reading performance (Deutsch et al., 2005; Niogi and McCandliss, 2006), it may be involved in the phonological processing of numbers when completing math tasks (van Eimeren et al., 2008). Alternatively, the superior corona radiata could be related to children's use of finger counting due to a shared neural representation between fingers and numbers (Matejko and Ansari, 2015). Children's use of finger counting strategies reduces over time (Peters and De Smedt, 2018) and may no longer be dominant by 13 years, however, it is possible that the repeated use of this strategy during development strengthens the shared neural pathways and they remain more permanently linked. Although the functional relevance of the sensorimotor tracts for math requires further investigation, we provide evidence that the development of axons in these tracts is important for children's math computation ability.

Further emphasising the importance of the sensorimotor network, we found that greater change over time in FDC in the posterior body of the corpus callosum from 7 to 13 years was associated with greater development in math computation ability in all children. Only one previous study has investigated math abilities in relation to FA changes over time in children, but this was conducted over an 8-week period only, investigating the effects of a tutoring program, and the DTI analysis focused specifically on the superior longitudinal fasciculus (Jolles et al., 2016). Thus, children with accelerated axonal development of the posterior body of the corpus callosum may experience greater development in math computation ability, possibly due to enhanced inter-hemispheric integration and efficiency of information transfer between motor and somatosensory cortices.

White matter microstructure and macrostructure in some cortico-thalamic and thalamo-cortical pathways were also associated with better math computation ability at both 7 and 13 years, including the anterior and posterior corona radiata, and the anterior thalamic radiations. In line with these findings, we have previously reported positive FA-math associations in the anterior and posterior corona radiata in this cohort of VPT and FT children (Collins et al., 2019; Kelly et al., 2016). Furthermore, higher FA in these regions has been observed in mathematically-gifted adolescents compared with controls (Navas-Sánchez et al., 2014) and reduced FA observed in the anterior thalamic radiations of children with dyscalculia, compared with controls (Rykhlevskaia et al., 2009). Further corroborating the importance of the thalamic connections for childhood math, we also found that FC and FDC of the somatosensory fibres passing into and within the thalami were associated with math computation at both 7 and 13 years. We therefore propose, in line with the dominant neuroanatomical model of mathematical cognition (Dehaene and Cohen, 1995), that the fibre-specific microstructure and macrostructure of the thalamic pathways play a vital role in children's math computation ability, possibly through the modulation of attention, memory and processing speed (Fama and Sullivan, 2015).

Two white matter tracts where we did not find converging evidence of associations with math compared to voxel-level analyses are the superior and inferior longitudinal fasciculi (Li et al., 2013; Rykhlevskaia et al., 2009; Tsang et al., 2009), even though our previous studies in this cohort have observed positive FA-math associations in both of these tracts (Collins et al., 2019; Kelly et al., 2016). While the lack of

associations in the current study was initially surprising, it is likely explained by our use of the fibre-specific FBA framework which has allowed us to differentiate between crossing white matter tracts. For example, the superior longitudinal fasciculus is a long association tract that crosses other tracts where we have identified positive associations in the current study, including the corticospinal tract and fibres of the posterior body of the corpus callosum (Mito et al., 2018) which extend into the corona radiata (Yakar et al., 2018). The inferior longitudinal fasciculus, on the other hand, is often difficult to separate from the inferior fronto-occipital fasciculus using voxel-level analyses, however, using FBA allowed us to more clearly differentiate these tracts and assign associations to the inferior fronto-occipital fasciculus, rather than the inferior longitudinal fasciculus. As such, it is possible that previous voxel-level analyses that report positive associations with the superior and inferior longitudinal fasciculi may be a reflection of crossing fibres. These distinctions, however, need future investigation and replication in other samples using fibre-specific frameworks.

Adjustment for ICV for FC and FDC sometimes did not change or slightly reduced the number of significant fixels (7-year analysis and longitudinal analysis) and sometimes more substantially reduced the number of significant fixels (13-year analysis), with associations in general more confined to sensorimotor tracts after ICV adjustment. This suggests findings for FC and FDC in these sensorimotor tracts are unlikely to have been driven by macroscopic brain differences, whereas findings in other parts of the brain may have been. Cross-sectional associations remained present in similar regions when children with an IQ < 70 were excluded, indicating that these associations were largely independent of general cognitive ability. However, longitudinal associations were no longer present, after excluding children with an IQ < 70, suggesting they may be influenced by general cognitive ability. One consideration when interpreting our sensitivity analyses excluding children with an IQ < 70, however, is the use of different IQ tests at 7 and 13 years. While the WASI 4-subtest full-scale IQ and the KBIT-2 composite score are highly correlated ($r = 0.81$; Kaufman and Kaufman, 2004), the increased number of children with an estimated IQ < 70 at 13 years ($n = 1$ at 7 years to $n = 9$ at 13 years) may be attributed to the application of different IQ measures across time points.

A major strength of our study is our large sample size, however, we do acknowledge that the FT sample was smaller than the VPT sample and we were possibly underpowered to detect birth group interactions due to the smaller FT sample size. Additionally, in future, segmenting and analysing individual fibre tracts would be beneficial for specifying effect sizes for specific tracts and may reveal more subtle group differences in specific fibre pathways. However, we believe a whole-brain approach is appropriate given evidence that VPT children rely on different white matter pathways to FT peers for other cognitive skills (Bruckert et al., 2019; Travis et al., 2016; Vollmer et al., 2017), which may be missed when focussing on specific tracts of interest. Application of the advanced FBA pipeline is another strength of our study, as this approach has been shown to provide more anatomically specific and biologically interpretable results compared with previous non-fibre-specific approaches (Dhollander et al., 2020; Mito et al., 2018), and also enabled us to examine both the microstructural and macrostructural properties of individual fibre populations. Our data is of high quality at both timepoints, however, there are two limitations that should be considered when interpreting the findings. Firstly, a subset of our 7-year scans were acquired with non-uniform gradient directions and after excluding this subset in sensitivity analyses, results at the 7-year timepoint were no longer significant, which could be related to the non-uniform gradient directions or a reduction in power due to the substantial reduction in sample size of nearly one-third, meaning these results should be interpreted with caution. Secondly, we acknowledge there were differences in the diffusion sequences used at each timepoint, which could affect the longitudinal analysis. While this limitation is common in long-term, longitudinal neuroimaging studies as technology and techniques improve over time, all sequences and processing in this

study were the same between the groups (Kelly et al., 2020). Future studies using identical image sequences over time are required to validate our results. Additionally, in the future, studies investigating brain white matter in conjunction with cortical morphology may provide a more complete picture of the brain structural-functional relationships underpinning math ability.

In conclusion, this study found evidence that the fibre density and cross-sectional area of specific visual, sensorimotor and cortico-thalamic tracts are associated with better math computation ability, and accelerated maturation of the posterior body of the corpus callosum is associated with greater development in math computation ability in late childhood. The underlying neural pathways for math computation are similar for children born VPT and FT.

Data availability statement

The datasets generated during and/or analysed during the current study are available from the corresponding author on reasonable request. The MRI data are not publicly available due to ethical restrictions.

Declaration of Competing Interest

The authors do not have any conflicts of interest to declare.

Acknowledgements

We are grateful to the children and families that continue to support our research. We also thank the Victorian Infant Brain Studies, Developmental Imaging and Melbourne Children's MRI Centre teams at the Murdoch Children's Research Institute and Royal Children's Hospital Melbourne for their expertise in designing and collecting the data.

Funding

This research was supported by the Australian Government Research Training Program Scholarship (to SEC), the Australian National Health Medical Research Council (NHMRC; Centre for Research Excellence 546519, 1060733 and 1153176; Project Grant237117, 491209 and 1066555; Senior Research Fellowship1081288 to PJA; Investigator Grant1176077 to PJA; Career Development Fellowships1085754 and 1160003 to DKT and 1141354 to JLYC, and; Early Career Fellowship1012236 to DKT), the Murdoch Children's Research Institute, the Royal Children's Hospital, the Royal Children's Hospital Foundation (RCH1000 to JYMY), the Department of Paediatrics at the University of Melbourne, and the Victorian Government's Operational Infrastructure Support Program. The funding organizations/sponsors had no role in the design and conduct of the study; collection, management, analysis, and interpretation of the data; preparation, review, or approval of the manuscript; and decision to submit the manuscript for publication.

Appendix A. Supplementary data

Supplementary material related to this article can be found, in the online version, at doi:<https://doi.org/10.1016/j.dcn.2021.100987>.

References

Aarnoudse-Moens, C.S., Weisglas-Kuperus, N., van Goudoever, J.B., Oosterlaan, J., 2009. Meta-analysis of neurobehavioral outcomes in very preterm and/or very low birth weight children. *Pediatrics* 124 (2), 717–728. <https://doi.org/10.1542/peds.2008-2816>.

Andersson, J.L.R., Sotiropoulos, S.N., 2016. An integrated approach to correction for off-resonance effects and subject movement in diffusion MR imaging. *Neuroimage* 125, 1063–1078. <https://doi.org/10.1016/j.neuroimage.2015.10.019>.

Andersson, J.L.R., Skare, S., Ashburner, J., 2003. How to correct susceptibility distortions in spin-echo echo-planar images: application to diffusion tensor imaging. *Neuroimage* 20 (2), 870–888. [https://doi.org/10.1016/s1053-8119\(03\)00336-7](https://doi.org/10.1016/s1053-8119(03)00336-7).

Andersson, J.L.R., Graham, M.S., Zsoldos, E., Sotiropoulos, S.N., 2016. Incorporating outlier detection and replacement into a non-parametric framework for movement and distortion correction of diffusion MR images. *Neuroimage* 141, 556–572. <https://doi.org/10.1016/j.neuroimage.2016.06.058>.

Andersson, J.L.R., Graham, M.S., Drobniak, I., Zhang, H., Filippini, N., Bastiani, M., 2017. Towards a comprehensive framework for movement and distortion correction of diffusion MR images: within volume movement. *Neuroimage* 152, 450–466. <https://doi.org/10.1016/j.neuroimage.2017.02.085>.

Arsalidou, M., Pawliw-Levac, M., Sadeghi, M., Pascual-Leone, J., 2018. Brain areas associated with numbers and calculations in children: meta-analyses of fMRI studies. *Dev. Cogn. Neurosci.* 30, 239–250. <https://doi.org/10.1016/j.dcn.2017.08.002>.

Basten, M., Jaekel, J., Johnson, S., Gilmore, C., Wolke, D., 2015. Preterm birth and adult wealth: mathematics skills count. *Psychol. Sci.* 26 (10), 1608–1619. <https://doi.org/10.1177/0956797615596230>.

Bastiani, M., Cottaar, M., Fitzgibbon, S.P., Suri, S., Alfaro-Almagro, F., Sotiropoulos, S.N., et al., 2018. Automated quality control for within and between studies diffusion MRI data using a non-parametric framework for movement and distortion correction. *Neuroimage*. <https://doi.org/10.1016/j.neuroimage.2018.09.073>.

Bhushan, C., Haldar, Justin P., Joshi, A.A., Leahy, R.M., 2012. Correcting susceptibility induced distortion in diffusion-weighted MRI using constrained nonrigid registration. Paper Presented at the Asia-Pacific Signal and Information Processing Association Annual Summit and Conference (Apsipa Asc). ISI&://WOS: 000319456200258.

Bruckert, L., Borchers, L.R., Dodson, C.K., Marchman, V.A., Travis, K.E., et al., 2019. White matter plasticity in reading-related pathways differs in children born preterm and at term: a longitudinal analysis. *Front. Hum. Neurosci.* 13 <https://doi.org/10.3389/fnhum.2019.00139>.

Cantlon, J.F., Libertus, M.E., Pinel, P., Dehaene, S., Brannon, E.M., Pelphrey, K.A., 2009. The neural development of an abstract concept of number. *J. Cogn. Neurosci.* 21 (11), 2217–2229. <https://doi.org/10.1162/jocn.2008.21159>.

Collins, S.E., Spencer-Smith, M., Mürner-Lavanchy, I.M., Kelly, C.E., Pyman, P., Pascoe, L., et al., 2019. White matter microstructure correlates with mathematics but not word reading performance in 13-year-old children born very preterm and full-term. *Neuroimage Clin.* 24, 101944. <https://doi.org/10.1016/j.nicl.2019.101944>.

Dehaene, S., Cohen, L., 1995. Towards an anatomical and functional model of number processing. *Mathematical Cognition*, pp. 83–120.

Dehaene, S., Piazza, M., Pinel, P., Cohen, L., 2003. Three parietal circuits for number processing. *Cogn. Neuropsychol.* 20 (3), 487–506. <https://doi.org/10.1080/02643290244000239>.

Deutsch, G.K., Dougherty, R.F., Bammer, R., Siok, W.T., Gabrieli, J.D.E., Wandell, B., 2005. Children's reading performance is correlated with white matter structure measured by diffusion tensor imaging. *Cortex* 41 (3), 354–363. [https://doi.org/10.1016/S0010-9452\(08\)70272-7](https://doi.org/10.1016/S0010-9452(08)70272-7).

Dhollander, T., et al., 2020. Fixel-based Analysis of Diffusion MRI: Methods, Applications, Challenges and Opportunities. OSFPreprints.

Dougherty, R.F., Ben-Shachar, M., Bammer, R., Brewer, A.A., Wandell, B.A., 2005. Functional organization of human occipital-callosal fiber tracts. *Proc. Natl. Acad. Sci. U. S. A.* 102 (20), 7350–7355. <https://doi.org/10.1073/pnas.0500003102>.

Fama, R., Sullivan, E.V., 2015. Thalamic structures and associated cognitive functions: relations with age and aging. *Neurosci. Biobehav. Rev.* 54, 29–37. <https://doi.org/10.1016/j.neubiorev.2015.03.008>.

Genc, S., Smith, R.E., Malpas, C.B., Anderson, V., Nicholson, J.M., Efron, D., et al., 2018. Development of white matter fibre density and morphology over childhood: A longitudinal fixel-based analysis. *Neuroimage* 183, 666–676. <https://doi.org/10.1016/j.neuroimage.2018.08.043>.

Gabner, R.H., Ansari, D., Koschutnig, K., Reishofer, G., Ebner, F., Neuper, C., 2009. To retrieve or to calculate? Left angular gyrus mediates the retrieval of arithmetic facts during problem solving. *Neuropsychologia* 47 (2), 604–608. <https://doi.org/10.1016/j.neuropsychologia.2008.10.013>.

Hofer, S., Frahm, J., 2006. Topography of the human corpus callosum revisited—comprehensive fiber tractography using diffusion tensor magnetic resonance imaging. *Neuroimage* 32 (3), 989–994. <https://doi.org/10.1016/j.neuroimage.2006.05.044>.

Jolles, D., Wassermann, D., Chokhani, R., Richardson, J., Tenison, C., Bammer, R., et al., 2016. Plasticity of left perisylvian white-matter tracts is associated with individual differences in math learning. *Brain Struct. Funct.* 221 (3), 1337–1351. <https://doi.org/10.1007/s00429-014-0975-6>.

Kaufman, A.S., Kaufman, N.L., 2004. Kaufman Brief Intelligence Test, second edition. Pearson, Inc., Bloomington, MN.

Kelly, C., E, Thompson, D., K, Chen, J., Leemans, A., Adamson, C.L., Inder, T.E., et al., 2016. Axon density and axon orientation dispersion in children born preterm. *Hum. Brain Mapp.* 37 (9), 3080–3102. <https://doi.org/10.1002/hbm.23227>.

Kelly, C.E., Thompson, D.K., Genc, S., Chen, J., Yang, J.Y., Adamson, C., et al., 2020. Long-term development of white matter fibre density and morphology up to 13 years after preterm birth: a fixel-based analysis. *Neuroimage* 220, 117068. <https://doi.org/10.1016/j.neuroimage.2020.117068>.

Klein, E., Moeller, K., Huber, S., Willmes, K., Kiechl-Kohlendorfer, U., Kaufmann, L., 2018. Gestational age modulates neural correlates of intentional, but not automatic number magnitude processing in children born preterm. *Int. J. Dev. Neurosci.* 65, 38–44. <https://doi.org/10.1016/j.ijdevneu.2017.10.004>.

Leemans, A., Jones, D.K., 2009. The B-matrix must be rotated when correcting for subject motion in DTI data. *Magn. Reson. Med.* 61 (6), 1336–1349. <https://doi.org/10.1002/mrm.21890>.

Li, Y., Hu, Y., Wang, Y., Weng, J., Chen, F., 2013. Individual structural differences in left inferior parietal area are associated with school children's arithmetic scores. *Front. Hum. Neurosci.* 7, 844. <https://doi.org/10.3389/fnhum.2013.00844>.

- Li, K., Sun, Z., Han, Y., Gao, L., Yuan, L., Zeng, D., 2015. Fractional anisotropy alterations in individuals born preterm: a diffusion tensor imaging meta-analysis. *Dev. Med. Child Neurol.* 57 (4), 328–338. <https://doi.org/10.1111/dmcn.12618>.
- Matejko, A.A., Ansari, D., 2015. Drawing connections between white matter and numerical and mathematical cognition: a literature review. *Neurosci. Biobehav. Rev.* 48, 35–52. <https://doi.org/10.1016/j.neubiorev.2014.11.006>.
- Matejko, A.A., Price, G.R., Mazzocco, M.M.M., Ansari, D., 2013. Individual differences in left parietal white matter predict math scores on the Preliminary Scholastic Aptitude Test. *Neuroimage* 66, 604–610. <https://doi.org/10.1016/j.neuroimage.2012.10.045>.
- Mito, R., Raffelt, D.A., Dhollander, T., Vaughan, D.N., Tournier, J.D., Salvado, O., et al., 2018. Fibre-specific white matter reductions in Alzheimer's disease and mild cognitive impairment. *Brain* 141 (3), 888–902. <https://doi.org/10.1093/brain/awx355>.
- Navas-Sánchez, F.J., Alemán-Gómez, Y., Sánchez-Gonzalez, J., Guzmán-De-Villoria, J.A., Franco, C., Robles, O., et al., 2014. White matter microstructure correlates of mathematical giftedness and intelligence quotient. *Hum. Brain Mapp.* 35 (6), 2619–2631. <https://doi.org/10.1002/hbm.22355>.
- Nichols, T.E., Holmes, A.P., 2002. Nonparametric permutation tests for functional neuroimaging: a primer with examples. *Hum. Brain Mapp.* 15 (1), 1–25. <https://doi.org/10.1002/hbm.1058>.
- Niogi, S.N., McCandliss, B.D., 2006. Left lateralized white matter microstructure accounts for individual differences in reading ability and disability. *Neuropsychologia* 44 (11), 2178–2188. <https://doi.org/10.1016/j.neuropsychologia.2006.01.011>.
- Nosarti, C., Nam, K.W., Walshe, M., Murray, R.M., Cuddy, M., Rifkin, L., Allin, M.P.G., 2014. Preterm birth and structural brain alterations in early adulthood. *Neuroimage Clin.* 6, 180–191. <https://doi.org/10.1016/j.nicl.2014.08.005>.
- Oishi, K., Faria, A.V., van Zijl, P.C.M., Mori, S., 2011. *MRI Atlas of Human White Matter*, 2nd ed. Elsevier B.V.
- Pannek, K., Fripp, J., George, J.M., Fiori, S., Colditz, P.B., Boyd, R.N., Rose, S.E., 2018. Fixel-based analysis reveals alterations in brain microstructure and macrostructure of preterm-born infants at term equivalent age. *Neuroimage Clin.* 18, 51–59. <https://doi.org/10.1016/j.nicl.2018.01.003>.
- Pannek, K., George, J.M., Boyd, R.N., Colditz, P.B., Rose, S.E., Fripp, J., 2020. Brain microstructure and morphology of very preterm-born infants at term equivalent age: associations with motor and cognitive outcomes at 1 and 2 years. *Neuroimage* 221, 117163. <https://doi.org/10.1016/j.neuroimage.2020.117163>.
- Parsons, S., Bynner, J., 2005. *Does Numeracy Matter More? (National Research and Development Centre for Adult Literacy and Numeracy)*. Retrieved from. Institute of Education, London.
- Pecheva, D., Tournier, J.D., Pietsch, M., Christiaens, D., Batalle, D., Alexander, D.C., et al., 2019. Fixel-based analysis of the preterm brain: disentangling bundle-specific white matter microstructural and macrostructural changes in relation to clinical risk factors. *Neuroimage Clin.* 23, 101820. <https://doi.org/10.1016/j.nicl.2019.101820>.
- Peters, L., De Smedt, B., 2018. Arithmetic in the developing brain: a review of brain imaging studies. *Dev. Cogn. Neurosci.* 30, 265–279. <https://doi.org/10.1016/j.dcn.2017.05.002>.
- Putnam, M.C., Steven, Megan S., Doron, Karl W., Riggall, Adam C., Gazzaniga, Michael S., 2010. Cortical projection topography of the human splenium: hemispheric asymmetry and individual differences. *J. Cogn. Neurosci.* 22 (8), 1662–1669.
- Raffelt, D.A., Tournier, J.D., Fripp, J., Crozier, S., Connelly, A., Salvado, O., 2011. Symmetric diffeomorphic registration of fibre orientation distributions. *Neuroimage* 56 (3), 1171–1180. <https://doi.org/10.1016/j.neuroimage.2011.02.014>.
- Raffelt, D.A., Tournier, J.D., Crozier, S., Connelly, A., Salvado, O., 2012. Reorientation of fiber orientation distributions using apodized point spread functions. *Magn. Reson. Med.* 67 (3), 844–855. <https://doi.org/10.1002/mrm.23058>.
- Raffelt, D.A., Smith, R.E., Ridgway, G.R., Tournier, J.D., Vaughan, D.N., Rose, S., et al., 2015. Connectivity-based fixel enhancement: Whole-brain statistical analysis of diffusion MRI measures in the presence of crossing fibres. *Neuroimage* 117, 40–55. <https://doi.org/10.1016/j.neuroimage.2015.05.039>.
- Raffelt, D.A., Tournier, J.D., Smith, R.E., Vaughan, D.N., Jackson, G., Ridgway, G.R., Connelly, A., 2017. Investigating white matter fibre density and morphology using fixel-based analysis. *Neuroimage* 144 (Part A), 58–73. <https://doi.org/10.1016/j.neuroimage.2016.09.029>.
- Rivera, S.M., Reiss, A.L., Eckert, M.A., Menon, V., 2005. Developmental changes in mental arithmetic: evidence for increased functional specialization in the left inferior parietal cortex. *Cereb. Cortex* 15 (11), 1779–1790. <https://doi.org/10.1093/cercor/bhi055>.
- Roberts, G., Howard, K., Spittle, A.J., Brown, N.C., Anderson, P.J., Doyle, L.W., 2008. Rates of early intervention services in very preterm children with developmental disabilities at age 2 years. *J. Paediatr. Child Health* 44 (5), 276–280. <https://doi.org/10.1111/j.1440-1754.2007.01251.x>.
- Rosenberg-Lee, M., Barth, M., Menon, V., 2011. What difference does a year of schooling make? Maturation of brain response and connectivity between 2nd and 3rd grades during arithmetic problem solving. *Neuroimage* 57 (3), 796–808. <https://doi.org/10.1016/j.neuroimage.2011.05.013>.
- Rykhlevskaia, E., Uddin, L.Q., Kondos, L., Menon, V., 2009. Neuroanatomical correlates of developmental dyscalculia: combined evidence from morphometry and tractography. *Front. Hum. Neurosci.* 3, 51. <https://doi.org/10.3389/fnhum.09.051.2009>.
- Shum, J., Hermes, D., Foster, B.L., Dastjerdi, M., Rangarajan, V., Winawer, J., et al., 2013. A brain area for visual numerals. *J. Neurosci.* 33 (16), 6709–6715. <https://doi.org/10.1523/JNEUROSCI.4558-12.2013>.
- Simms, V., Gilmore, C., Cragg, L., Clayton, S., Marlow, N., Johnson, S., 2015. Nature and origins of mathematics difficulties in very preterm children: a different etiology than developmental dyscalculia. *Pediatr. Res.* 77 (2), 389–395. <https://doi.org/10.1038/pr.2014.184>.
- Smith, S.M., 2002. Fast robust automated brain extraction. *Hum. Brain Mapp.* 17 (3), 143–155. <https://doi.org/10.1002/hbm.10062>.
- Smith, R.E., Tournier, J.D., Calamante, F., Connelly, A., 2013. SIFT: spherical-deconvolution informed filtering of tractograms. *Neuroimage* 67, 298–312. <https://doi.org/10.1016/j.neuroimage.2012.11.049>.
- Smith, R.E., Dhollander, T., Connelly, A., 2019. On the regression of intracranial volume in fixel-based analysis. Paper Presented at the ISMRM.
- StataCorp, 2019. *Stata Statistical Software: Release 16*. StataCorp LLC., College Station, TX.
- Thompson, D.K., Lee, K.J., Egan, G.F., Warfield, S.K., Doyle, L.W., Anderson, P.J., Inder, T.E., 2014. Regional white matter microstructure in very preterm infants: predictors and 7 year outcomes. *Cortex* 52, 60–74. <https://doi.org/10.1016/j.cortex.2013.11.010>.
- Tournier, J.D., Calamante, F., Connelly, A., 2013. Determination of the appropriate b value and number of gradient directions for high-angular-resolution diffusion-weighted imaging. *NMR Biomed.* 26 (12), 1775–1786. <https://doi.org/10.1002/nbm.3017>.
- Tournier, J.D., Smith, R., Raffelt, D.A., Tabbara, R., Dhollander, T., Pietsch, M., et al., 2019. MRtrix3: a fast, flexible and open software framework for medical image processing and visualisation. *Neuroimage* 202, 116137. <https://doi.org/10.1016/j.neuroimage.2019.116137>.
- Travis, K.E., Ben-Shachar, M., Myall, N.J., Feldman, H.M., 2016. Variations in the neurobiology of reading in children and adolescents born full term and preterm. *Neuroimage Clin.* 11, 555–565. <https://doi.org/10.1016/j.nicl.2016.04.003>.
- Tsang, J.M., Dougherty, R.F., Deutsch, G.K., Wandell, B.A., Ben-Shachar, M., 2009. Frontoparietal white matter diffusion properties predict mental arithmetic skills in children. *Proc. Natl. Acad. Sci. U. S. A.* 106 (52), 22546–22551. <https://doi.org/10.1073/pnas.0906094106>.
- Tustison, N.J., Avants, B.B., Cook, P.A., Zheng, Y., Egan, A., Yushkevich, P., Gee, J.C., 2010. N4ITK: improved N3 bias correction. *IEEE Trans. Med. Imaging* 29 (6), 1310–1320. <https://doi.org/10.1109/TMI.2010.2046908>.
- Twilhaar, E.S., de Kieviet, J.F., Aarnoudse-Moens, C.S., van Elburg, R.M., Oosterlaan, J., 2018. Academic performance of children born preterm: a meta-analysis and meta-regression. *Arch. Dis. Child. - Fetal Neonatal Ed.* 103 (4), F322–F330. <https://doi.org/10.1136/archdischild-2017-312916>.
- van Eimeren, L., Niogi, S.N., McCandliss, B.D., Holloway, I.D., Ansari, D., 2008. White matter microstructures underlying mathematical abilities in children. *Neuroreport* 19 (11), 1117–1121.
- Vangberg, T.R., Skranes, J., Dale, A.M., Martinussen, M., Brubakk, A.-M., Haraldseth, O., 2006. Changes in white matter diffusion anisotropy in adolescents born prematurely. *Neuroimage* 32 (4), 1538–1548. <https://doi.org/10.1016/j.neuroimage.2006.04.230>.
- Vollmer, B., Lundequist, A., Mårtensson, G., Nagy, Z., Lagercrantz, H., Smedler, A.-C., Forssberg, H., 2017. Correlation between white matter microstructure and executive functions suggests early developmental influence on long fibre tracts in preterm born adolescents. *PLoS One* 12 (6). <https://doi.org/10.1371/journal.pone.0178893>.
- Wechsler, D., 1999. *Wechsler Abbreviated Scale of Intelligence (WASI), first ed.* Psychological Corporation, San Antonio, TX.
- Wilkinson, G.S., Robertson, G.J., 2006. *Wide Range Achievement Test 4. Psychological Assessment Resources*, Lutz, FL.
- Wilson-Ching, M., Pascoe, L., Doyle, L.W., Anderson, P.J., 2014. Effects of correcting for prematurity on cognitive test scores in childhood. *J. Paediatr. Child Health* 50 (3), 182–188. <https://doi.org/10.1111/jpc.12475>.
- Yakar, F., Eroglu, U., Peker, E., Armagan, E., Comert, A., Ugur, H.C., 2018. Structure of corona radiata and tapetum fibers in ventricular surgery. *J. Clin. Neurosci.* 57, 143–148. <https://doi.org/10.1016/j.jocn.2018.08.041>.
- Zhang, H., Schneider, T., Wheeler-Kingshott, C.A., Alexander, D.C., 2012. NODDI: practical in vivo neurite orientation dispersion and density imaging of the human brain. *Neuroimage* 61 (4), 1000–1016. <https://doi.org/10.1016/j.neuroimage.2012.03.072>.